Tracking of Transplanted Human Mesenchymal Stem Cells in Living Mice using Near-Infrared Ag_2S Quantum Dots

*Guangcun Chen, Fei Tian, Yan Zhang, Yejun Zhang, Chunyan Li, and Qiangbin Wang**

Stem cell therapeutics has emerged as a novel regenerative therapy for tissue repair in the last decade. However, dynamically tracking the transplanted stem cells in vivo remains a grand challenge for stem cell-based regeneration medicine in full understanding the function and the fate of the stem cells. Herein, Ag_2S quantum dots (QDs) in the second near-infrared window (NIR-II, 1.0–1.4 μm) are employed for dynamically tracking of human mesenchymal stem cells (hMSCs) in vivo with high sensitivity and high spatial and temporal resolution. As few as 1000 Ag_2S QDs-labeled hMSCs are detectable in vivo and their fluorescence intensity can maintain up to 30 days. The in situ translocation and dynamic distribution of transplanted hMSCs in the lung and liver can be monitored up to 14 days with a temporal resolution of 100 ms. The in vivo high-resolution imaging indicates the heparin-facilitated translocation of hMSCs from lung to liver as well as the long-term retention of hMSCs in the liver contribute to the treatment of liver failure. The novel NIR-II imaging offers a possibility of tracking stem cells in living animals with both high spatial and temporal resolution, and encourages the future clinical applications in imaging-guided cell therapies.

1. Introduction

Stem cells have shown great potential in clinical applications, such as cardiac repair, bone regeneration, and treatment of liver diseases.[1–5] However, the migration behaviors, engraftment efficiency and functionality of transplanted stem cells in living animal model are poorly understood. Thus, the development of high-resolution imaging techniques to monitor the temporal and spatial homing of transplanted stem cells to target tissues in living animal model is urgently needed for a better understanding of both the therapeutic mechanisms and the safety issues of stem cells before their uses in clinical trials.

Ideal stem cell tracking technique should be noninvasive, highly sensitive, and capable of tracking stem cells at any desired time and at any anatomic location in the live animal.[6] The current methodologies, inculding report gene of green fluorescent protein (GFP) or luciferase,[7–9] quantum dots (QDs),[10,11] upconversion nanoparticles (UCNPs),[12–14] magnetic resonance imaging (MRI),[9,15–17] and positron emission tomography (PET),[18] and so forth, have been extensively employed in stem cell research to identify the transplanted stem cells in vivo. Unfortunately, none of these imaging techniques meets the requirement of high sensitivity, high temporal and spatial resolution in in vivo imaging. Recently, it is reported that fluorescence imaging in the second near-infrared window (NIR-II, 1.0–1.4 μm) is an ideal strategy for in vivo imaging due to its reduced photon scattering and lower autofluorescence, and thus deeper tissue penetration in comparison with the fluorescence imaging in visible and the first near-infrared window (NIR-I, 650-950 nm).[19,20] For example, NIR-II emitting agents such as single-walled nanotubes (SWNTs) and Ag_2S QDs have been successfully used for mouse hind limb vasculatures imaging and tumor detection with an ultra-high spatial resolution of 30 μm and a temporal resolution of less than 50 ms, which is unattainable by the traditional fluorescence imaging or tomographic imaging such as MRI and PET.[21,22]

In this work, for the first time, Ag_2S QDs with high fluorescence quantum yield (15.5%, approximate 5 fold of SWNTs) and high biocompatibility[23–25] were employed for high-efficiency labeling and tracking of human mesenchymal stem cells (hMSCs) in vivo. The chemical stability, photostability, and possible cytotoxicity of Ag_2S QDs in stem cells were systematically studied, and then in vivo imaging of the translocation and organ-specific accumulation of transplanted hMSCs in mice with liver failure was performed. The study demonstrates the high chemical stability, photostability and biocompability nature of Ag_2S QDs, which is desirable for stem cell labeling. Moreover, this novel technique opens up a possibility of tracking transplanted stem cells in living animals with both high sensitivity and high spatial resolution, and enables its real-time imaging and long-term tracking.

2. Results and Discussion

2.1. Labeling of hMSCs with Tat-Ag_2S QDs

In order to image the transplanted hMSCs in vivo, Ag_2S QDs were firstly conjugated with Tat peptide as the targeting ligand

Dr. G. Chen, F. Tian, Y. Zhang, Y. J. Zhang,
Dr. C. Li, Prof. Q. Wang
Suzhou Key Laboratory of
Nanobiomedical Characterization
Division of Nanobiomedicine and *i*-Lab
Suzhou Institute of Nano-Tech and Nano-Bionics
Chinese Academy of Sciences
Suzhou, 215123, China
E-mail: qbwang2008@sinano.ac.cn

DOI: 10.1002/adfm.201303263

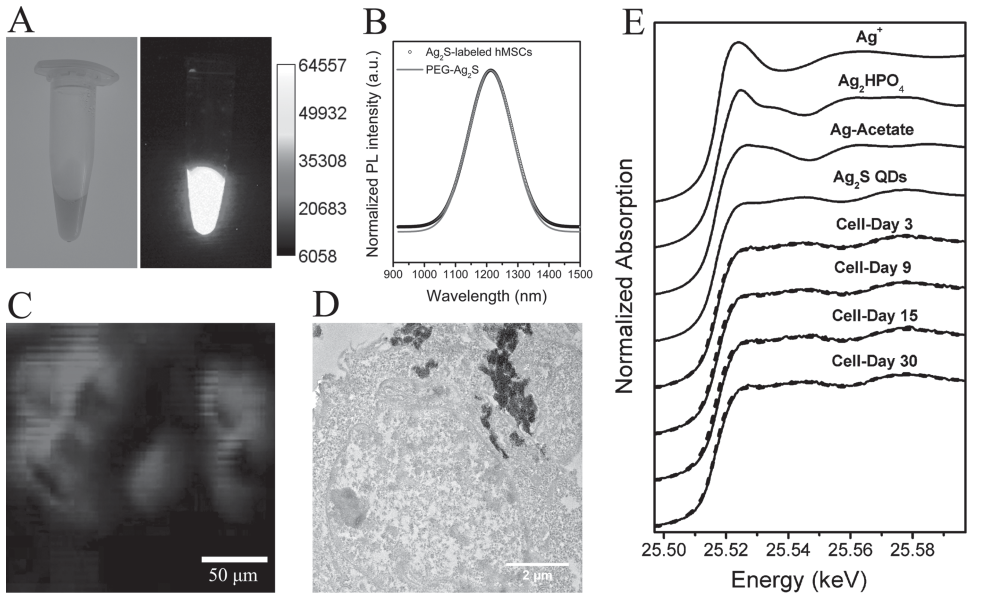

Figure 1. Labeling of hMSCs with Tat-Ag_2S QDs. A) A photoluminescence (PL) image of the Ag_2S QDs-labeled hMSCs solution at a density of 4×10^6 cell mL^{-1}. B) The NIR PL spectra of Ag_2S QDs-labeled hMSCs (black circle) and PEG-Ag_2S QDs (red line). C) NIR-II PL images of Ag_2S QDs-labeled hMSCs from a NIR confocal laser scanning microscope. D) TEM images of Ag_2S QDs-labeled hMSCs, black arrows indicate the Ag_2S QDs aggregate in the cytoplasm of hMSCs. E) Ag XANES spectra of the Ag_2S QDs-labeled hMSCs after 3, 9, 15, and 30 days incubation and the reference compounds of Ag_2S QDs, Ag-acetate, Ag_2HPO_4, and Ag^+. The black solid lines show the data. The black broken lines show the fit with data sets of model compounds.

to hMSCs (Supporting Information Figure S1,S2). After incubation of hMSCs in a low glucose-Dulbecco's modified Eagle medium (L-DMEM) containing 12.5 μg mL^{-1} of Tat-Ag_2S QDs for 12 h, the hMSCs were detected with strong NIR emission both in their bulk solution (**Figure 1**A) and at single cell level (Figure 1C) by an InGaAs CCD camera and NIR confocal laser scanning microscope (CLSM), respectively. Moreover, the NIR fluorescence spectra of Ag_2S QDs conjugated with polyethylene glycol (PEG–Ag_2S) and Ag_2S QDs-labeled hMSCs exhibited identical emission curves and peak positions (Figure 1B). Transmission electron microscope (TEM) observation further confirms the effective labeling of Ag_2S QDs in hMSCs as Ag_2S QDs were predominately located in the cytoplasm of cells without penetrating into the nucleus (Figure 1D). These results demonstrated hMSCs were effectively labeled by Tat-Ag_2S QDs.

It has been known that the toxicity of metal-contained nanomaterials presumably resulted from the degradation of nanomaterials by releasing toxic metal ions.[26] For the most widely used CdSe@ZnS and CdTe QDs, the released cadmium ions in biological system are proved to be responsible for their cytotoxicity.[27,28] Thus, the chemical stability of Ag_2S QDs in hMSCs was then examined by using the synchrotron radiation X-ray absorption near-edge structure (XANES) spectrum, in which the hMSCs labeled with Ag_2S QDs from 3 days up to 30 days were analyzed, to reveal the fate of Ag_2S in hMSCs (Figure 1E). It is supposed that, if the degradation of Ag_2S QDs within hMSCs happened, Ag^+ will be released and partially be chelated by cell-rich carboxyl and phosphoryl groups. Thereby, Ag^+, Ag-Acetate, Ag_2HPO_4, and Ag_2S QDs were chosen as the reference compounds, while Ag_2S QDs-labeled hMSCs that grown for 3, 9, 15, and 30 days were chosen as the tested samples, respectively. As shown in Figure 1E, the XANES spectra of Ag-Acetate, Ag_2HPO_4, Ag^+, and Ag_2S QDs are different from one another. Surprisingly, no discernible changes of XANES spectra of Ag_2S were observed for the Ag_2S QDs-labeled hMSCs at 3, 9, 15, and 30 days and all the spectra were similar to that of the Ag_2S QDs reference. To quantitatively analyze the chemical species of Ag in cells, the Ag XANES spectra of Ag_2S QDs-labeled hMSCs were fitted with a linear combination of the XANES spectra of Ag-Acetate, Ag_2HPO_4, Ag^+, and Ag_2S QDs by using the LSFitXAFS program. It was found that Ag_2S QDs-labeled hMSCs represent 100% of Ag_2S species in all hMSCs samples without release of free Ag^+ (Supporting Information Table S1). These results indicated the extremely high chemical stability of Ag_2S QDs in intracellular environment, which promises the high photostability and high biocompatibility of Ag_2S QDs for long-term in vivo imaging.

2.2. Interactions of Tat-Ag_2S QDs with hMSCs

Although the cytotoxicity of Ag_2S QDs on mouse fibroblast L929 cell line has been fully examined,[24] this assay is carried out to evaluate the cytotoxicity of Ag_2S QDs on the labeled hMSCs because hMSCs are more sensitive to the exterior stimulus. 5-ethynyl-20-deoxyuridine (EdU) incorporation assay was firstly performed to characterize the proliferation of hMSCs after 24 h treatment with Tat-Ag_2S QDs. As shown in **Figure 2**A and Supporting Information Figure S4, no statistical variation was observed for the hMSCs treated with Tat-Ag_2S QDs from 0 to 50 μg mL^{-1}. Furthermore, no appreciable delay effect of Ag_2S QDs on the long-term proliferation of hMSCs was observed up to 14 days (Supporting Information Figure S3). These results indicated that Tat-Ag_2S QDs has negligible side effect on the cell proliferation.

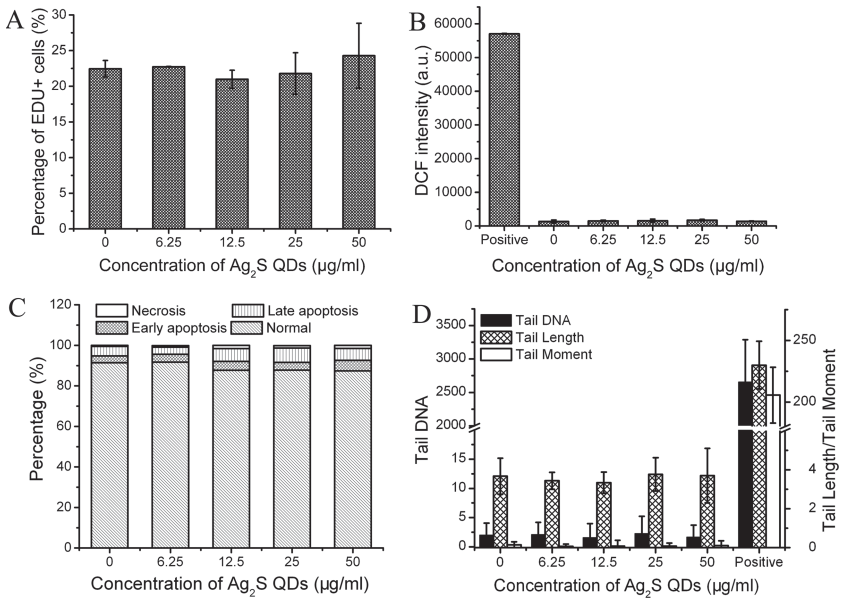

Figure 2. Cytotoxicity assays of Tat-Ag_2S QDs for hMSCs. A) Cell proliferation, B) ROS generation, C) apoptosis and necrosis, and D) DNA damage assays of hMSCs treated with 0, 6.25, 12.5, 25, and 50 μg mL^{-1} of Tat-Ag_2S for 24 h. Rosup (50 μg mL^{-1}) and H_2O_2 (10 μM) treated cells were used as positive controls in ROS and DNA damage assays, respectively. Data are expressed as mean ± standard error of three determinations.

It has been reported that QDs are able to induce oxidative stress by generating reactive oxygen species (ROS).[29] In this study, the formation of ROS induced by Tat-Ag_2S QDs exposure was studied via quantifying the fluorescence intensity of 20,70-dichlorofluorescein (DCF) by flow cytometry. It was found that hMSCs treated with ROSup as the positive control exhibited high intensity of DCF fluorescence. In contrast, the hMSCs treated with Tat-Ag_2S QDs in different concentrations showed much less DCF fluorescence (Figure 2B and Supporting Information Figure S5), suggesting minimum ROS induced by Tat-Ag_2S QDs treatment.

To assess the potential apoptosis and necrosis of hMSCs induced by Tat-Ag_2S QDs, cell staining with anti-annexin V-FITC and PI was carried out. No significant increase of apoptosis and necrosis cells in Tat-Ag_2S QDs-treated hMSCs was observed in comparison with the untreated hMSCs (Figure 2C and Supporting Information Figure S6), indicating the good biocompatibility of Tat-Ag_2S QDs.

To further evaluate the potential DNA damage caused by Tat-Ag_2S QDs, the single-cell gel electrophoresis assay (comet assay) was performed. The levels of DNA damage was indicated by the percent of DNA in the tail (tail DNA), tail length and tail moment. It was found that the levels of tail DNA, tail length and tail moment for Tat-Ag_2S QDs-treated and untreated hMSCs were quite similar and were much lower than that of the positive control treated with H_2O_2 (Figure 2D and Supporting Information Figure S7). These results indicated the negligible genotoxicity of Tat-Ag_2S QDs on hMSCs.

As stem cells, the differentiation capability of hMSCs is the most important character which makes them central in regenerative medicine. To investigate the potential adverse effects of Ag_2S QDs on the differentiation capacity of hMSCs, adipogenic and osteogenic differentiation assays were performed. Following adipogenic differentiation, oil-red O staining of hMSCs revealed the formation of lipid vacuole both in Ag_2S QDs-labeled and unlabeled hMSCs (**Figure 3**A). The quantification of oil-red O extracted from adipogenic cells at 404 nm absorbance further revealed similar levels of adipogenic differentiation between unlabeled and Ag_2S QDs-labeled hMSCs (Figure 3C). For osteogenic differentiation assay, hMSCs were treated with osteogenic supplements for 21 days, and detected by alizarin red staining. It was found that both unlabeled and Ag_2S QDs-labeled hMSCs were positive for alizarin red staining (Figure 3B). Moreover, colorimetric quantification of alizarin red extracted from osteogenic cells revealed the similar levels of osteogenic differentiation between unlabeled and Ag_2S QDs-labeled hMSCs (Figure 3D). These results indicated the differentiation capacity of hMSCs was not inhibited by Ag_2S QDs.

2.3. In Vivo Tracking of Ag_2S QDs-Labeled hMSCs in Mice

To dynamically track the hMSCs in vivo, high sensitivity is a prerequisite. Therefore, the in vivo detection sensitivity of Ag_2S QDs-labeled hMSCs by NIR in vivo imaging system was determined. Different numbers (1000, 10 000, 20 000, and 100 000) of hMSCs labeled with Ag_2S QDs were subcutaneously injected into the back of a nude mouse, respectively. Then the NIR fluorescence images were collected immediately or 3, 5, 8, 15, 20, and 30 days after cell injection, respectively (**Figure 4**A). Surprisingly, as few as 1000 Ag_2S-labeled hMSCs could be recognized using our in vivo imaging system and no significant decrease of NIR fluorescence intensity was observed for up to 30 days after subcutaneous transplantation (Figure 4B, D). This detection limit is much better than using QDs emitting in the visible region (CdSe@ZnS 655) as fluorophore, which could resolve no fewer than 50 000 cells subcutaneously transplanted beneath the skin of mice.[30] Recently, a spectacular detection limit as low as 10 stem cells had been achieved for in vivo cell imaging using UCNPs as probe.[13,14] However, a higher laser power density (400 mW cm^{-2}) and a longer exposure time (20 s),[13,14] as well as the overheating effect of 980 nm laser irradiation,[31] may deter the dynamic tracking of hMSCs in vivo as Ag_2S QDs. Additionally, the NIR fluorescence intensities of Ag_2S QDs-labeled hMSCs at each time point were also collected. A good linear relationship between cell number and the NIR fluorescence intensity were obtained, with a R^2 of 0.99 for in vivo imaging (Figure 4C). These results suggested the great potential of Ag_2S QDs in long-term stem cell tracking with high sensitivity. It is worth noting that the dilution of nanoparticles inside cells may limit the use of external labels for long-term stem cell tracking. Although Rosen et al. successfully tracked exogenous hMSCs in histologic sections with QDs for at least

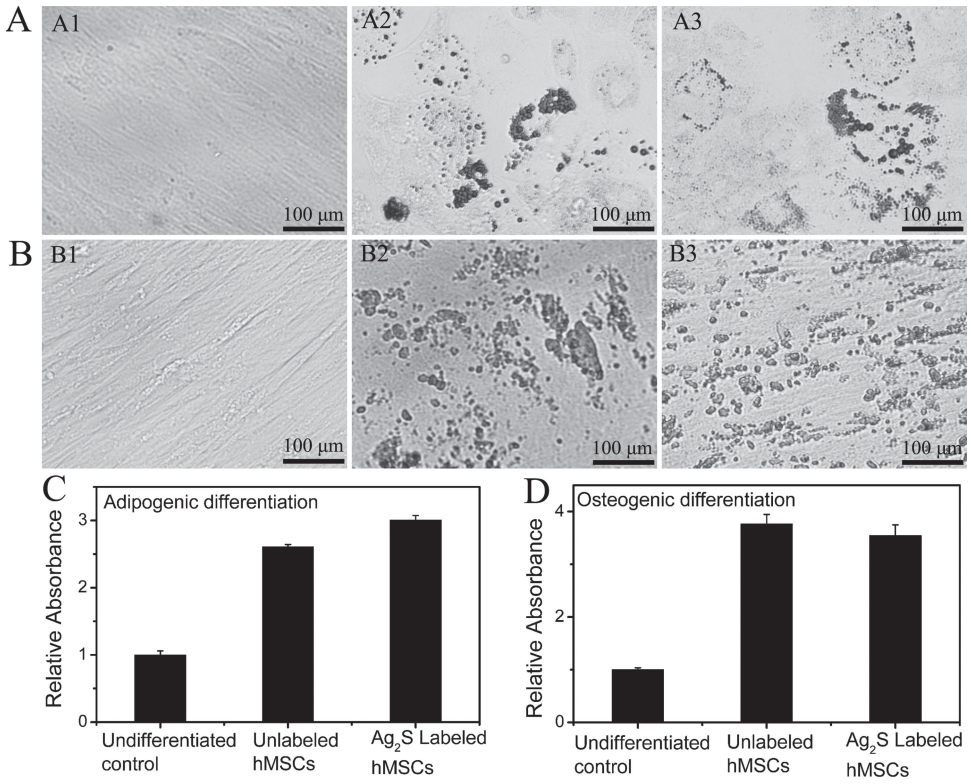

Figure 3. Effects of Ag_2S QDs on A) adipogenic and B) osteogenic differentiation of hMSCs. hMSCs was labeled with 12.5 μg mL^{-1} of Tat-Ag_2S QDs for 12 h and supplied with adipogenic medium for 14 days or osteogenic medium for 21 days. Non-differentiated hMSCs (A1) and adipogenic differentiated hMSCs A2) without or A3) with Ag_2S QDs-labeling were stained by oil-red O. B1) Non-differentiated hMSCs and osteogenic differentiated hMSCs B2) without or B3) with Ag_2S QDs-labeling were stained by alizarin red. Quantification of C) adipogenic and D) osteogenic differentiation by measuring the absorbance of oil-red O and alizarin red extracted from cell lysates at 404 nm, respectively. Data are expressed as mean ± standard error of three determinations.

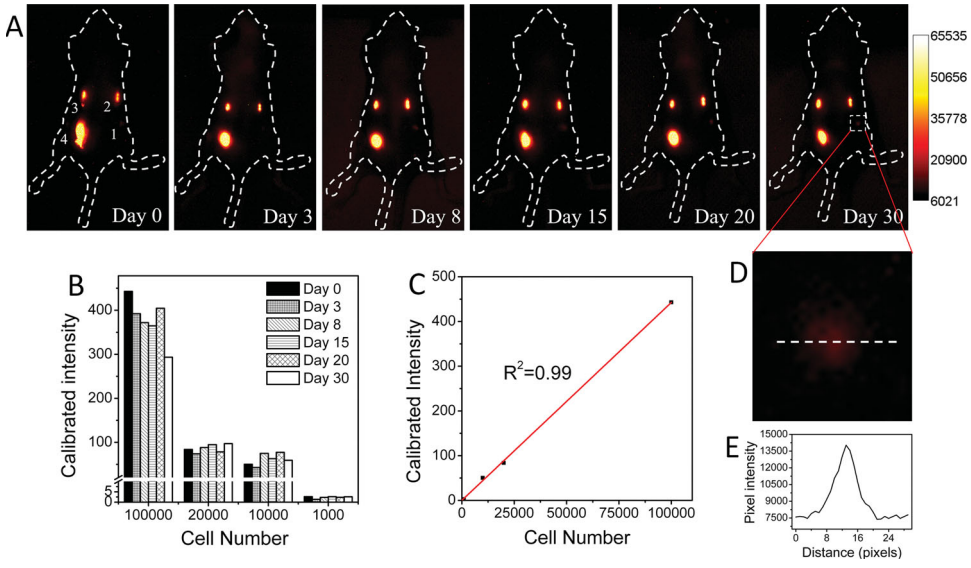

Figure 4. In vivo detection sensitivity of Ag_2S QDs-labeled hMSCs. A) PL images of a mouse subcutaneously injected with 1) 1000, 2) 10 000, 3) 20 000, and 4) 100 000 Ag_2S QDs-labeled hMSCs after 0-30 days post injection. B) Quantification of PL intensity of Ag_2S QDs-labeled hMSCs at different cell number after 0–30 days post injection. C) The linear relationship between cell numbers and total NIR fluorescent intensity in vivo imaging shown in (A). D) High magnification NIR PL image of 1000 Ag_2S QDs-labeled hMSCs after 30 days post injection. E) A cross-sectional fluorescence intensity profile measured along the white dashed line in (D).

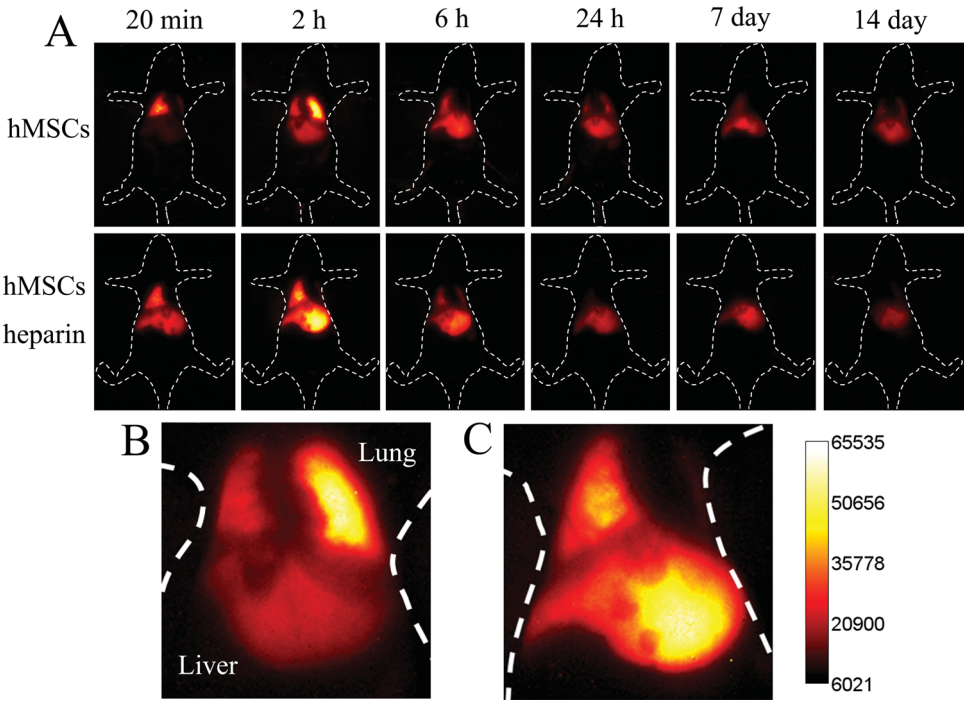

Figure 5. In vivo tracking of intravenously injected hMSCs in mice. A) The time course of the in vivo NIR PL images of a healthy mouse after transplantation of Ag_2S QDs-labeled hMSCs and a mouse with acute liver failure after transplantation of Ag_2S QDs-labeled hMSCs in combination with heparin at different times (20 min-14 days). B) Higher magnification NIR PL image of mice transplanted with hMSCs only after 2 h. C) Higher magnification NIR PL image of liver failure mice transplanted with hMSCs in combination with heparin after 2 h.

8 weeks following delivery and permit,[10] an ideal approach for long-term cell fate tracking in vivo will be the combination of external labels and report gene of luciferase for simultaneously imaging the translocation and physiological status of transplanted stem cells.

Previous reports have well documented the wide clinical applications of hMSCs in cardiac repair, bone regeneration and treatment of liver diseases.[1–5] However, direct evidence of the cell tracking in vivo is lack due to the inaccessibility of imaging technique with both high spatial and temporal resolution. By using the highly fluorescent, chemically stable and biocompatible Ag_2S QDs, for the first time, we clearly observed the whole-body translocation of hMSCs in mice at both high spatial and temporal resolution. As shown in **Figure 5**, in a mouse with acute liver failure, bright NIR fluorescence was clearly observed in the lung and liver of mice without requiring laparotomy after transplantation of the Ag_2S QDs-labeled hMSCs through tail vein injection. It is notable that the NIR fluorescence images could be obtained with an exposure time of 100 ms, offering the real-time in vivo imaging of Ag_2S QDs.

It has been reported that heparin can help the hMSCs pass through the capillaries in the lung to accumulate in the liver, which contributes to the liver failure treatment.[3,11] To further understand the effect of heparin on translocation of hMSCs, a long-term monitoring of transplanted hMSCs in mice was performed up to 14 days (Figure 5A). At the begin of 20 mins post transplantation of the Ag_2S labeled-hMSCs, it was found that, for the mouse transplanted with Ag_2S labeled-hMSCs alone, NIR signals were predominantly found in the lung. Whereas in combination with heparin, the strong NIR signals of Ag_2S QDs were detected in the liver instead of lung. At 2 h post transplantation, Ag_2S labeled-hMSCs were migrated from lung to liver as more NIR fluorescence signals observed in the liver. Again, the fluorescence intensity in the liver of the mouse injected with heparin is higher than that of the mouse without injection of heparin (Figure 5B,C). These findings demonstrated that heparin accelerated the translocation of hMSCs from lung to liver at the initial transplantation. However, the heparin did not enhance the retention of hMSCs in the liver as the NIR fluorescence signals in the two mice were getting similar at 24 h post injection regardless the use of heparin or not (Figure 5A). It is worth stating that fluorescence imaging in the NIR-II region offers desired tissue penetration depth due to the negligible photon scattering and minimal autofluorescence,[19] the fine distribution of hMSCs in the left lung, right lung and liver could be clearly distinguished as shown in the higher magnification NIR PL images of mice transplanted with hMSCs after 2 h (Figure 5B,C). These results suggested the great potential of Ag_2S QDs in stem cell tracking in living animals with both high temporal and spatial resolution.

To investigate the therapeutic potential of hMSCs for mice with acute liver failure, the liver histology analyses were conducted. Livers from mice with acute liver failure with and without hMSCs transplantation were harvested 24 h after transplantation and stained by hematoxylin and eosin. As shown in **Figure 6**, the liver histology from healthy mice showed uniform cellular morphology (Figure 6A), while there were a lot of light staining areas in injured liver, indicating the necrosis and

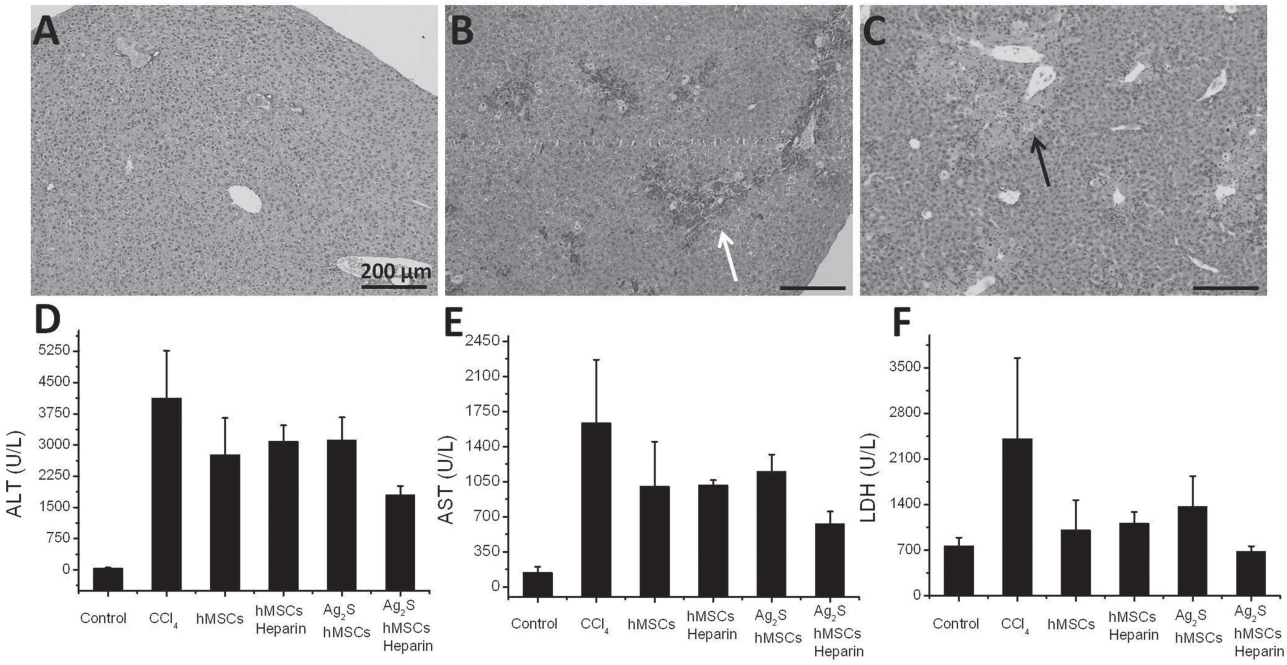

Figure 6. The liver histology and blood biochemistry analysis. A–C) Hematoxylin and eosin (HE) staining of histological sections of the livers from mice with A) normal livers, B) acute liver failure, or C) acute liver failure transplanted with hMSCs in combination with heparin for 24 h. White arrows indicate the accumulation of inflammatory cells in the areas with damaged hepatocytes. Black arrows indicate the necrosis and apoptosis of hepatocytes induced by CCl_4 injection. D–F) Concentration of liver failure markers such as D) ALT, E) AST, and F) LDH in blood serum of mice after hMSCs transplantation.

apoptosis of hepatocytes induced by CCl_4 injection (Figure 6B,C). Moreover, accumulation of inflammatory cells was observed in the areas with damaged hepatocytes. In contrast, there were much fewer inflammatory cells in the liver histology of mice transplanted with hMSCs in combination with heparin. The blood biochemistry assay further revealed the level of asparate aminotransferase (AST), alanine aminotransferase (ALT), and lactate dehydrogenase (LDH) increased distinctly in mice with CCl_4 injury, while the hMSCs transplantation decreased the level of AST, ALT, and LDH (Figure 6D,E,F). These results suggested a reduction of inflammatory cytokine accumulation in mice and an improvement of liver function by transplanted hMSCs. The paracrine effects of MSCs, such as secretion of immunosuppressors and promoters of regeneration, are thought to contribute to liver regeneration.[4] Additionally, similar therapeutic capability of hMSCs without or with Ag_2S QDs-labeling for decreasing the level of AST, ALT, and LDH were observed, which further proves the negligible toxicity of Ag_2S QDs.

3. Conclusion

In conclusion, Ag_2S QDs are a novel kind of fluorescent probes for tracking transplanted hMSCs in living mice. Conjugated with a Tat peptide, Ag_2S QDs can label hMSCs effectively, without causing of ROS production, apoptosis/necrosis and DNA damage in hMSCs or affecting the proliferation and differentiation of hMSCs and their therapeutic abilities for liver failure. High chemical stability and photostability of Ag_2S QDs in the cellular environment up to 30 days are observed, encouraging the applications of Ag_2S QDs for long-term cell tracking. Because of the negligible autofluorescence of live tissues in the NIR-II region, as few as 1000 cells are able to be detected for in vivo imaging, which is a significant improvement from traditional QDs-based cell tracking techniques in the visible and NIR-I region. For the first time, the in situ translocation and fine distribution of transplanted hMSCs in the lung and liver can be monitored up to 14 days with a temporal resolution less than 100 ms. The in vivo high-resolution fluorescence image results witness the facilitated translocation of hMSCs from lung to liver by heparin and the resulted high concentration of hMSCs in liver contributes to the treatment of liver failure. Our results highlight the promise of Ag_2S QDs as a NIR-II nanoprobe for long-term, noninvasive, in vivo stem cell tracking with both high sensitivity and elevated spatial and temporal resolution, and encourage further clinical applications in imaging-guided cell therapies.

4. Experimental Section

Conjugation of PEG-Ag_2S QDs with Tat Peptide: Highly water soluble PEG-Ag_2S QDs was prepared by coating Ag_2S QDs with amine-functionalized six-armed PEG as described in previous study.[22] The PEG-Ag_2S QDs were conjugated to Tat peptide through covalent bonding by using the cross linking reagent Sulfo-SMCC (Sigma).[32] The detailed illustration of Tat-Ag_2S QDs preparation was supplied in supporting information.

hMSCs Labeled with Tat-Ag_2S QDs: hMSCs were incubated with L-DMEM media containing 12.5 μg mL^{-1} Tat-Ag_2S QDs for 12 h. At the

end of incubation, hMSCs were repetitively washed with PBS to remove unbound Ag_2S QDs. Ag_2S QDs-labeled hMSCs were harvested and resuspended in PBS at a density of 4×10^6 cells mL^{-1}. The NIR-II PL images of hMSCs solution were collected using the NIR in vivo imaging system with an external 808 nm laser diode as the excitation source. The emission was collected by a NIR CCD camera from 1100–1700 nm with an exposure time of 50 ms. The Ag_2S QDs-labeled hMSCs were also imaged under a NIR CLSM using a 808 nm external laser as the excitation source. To further confirm the sub-cellular location of Ag_2S QDs in hMSCs, Ag_2S QDs-labeled hMSCs were analyzed under Tecnai G2 F20 S-Twin transmission electron microscopy (TEM).

X-Ray Absorption Fine Structure (XAFS) Analyses of Tat-Ag_2S QDs in hMSCs: For XAFS analyses, Ag_2S QDs-labeled hMSCs were incubated with fresh L-DMEM media for additional 3, 9, 15, and 30 days. The Ag XAFS spectra of cell samples and reference samples of Ag-Acetate, Ag_2HPO_4, Ag^+, and PEG-Ag_2S QDs were collected at beam line 14W1 of the Shanghai Synchrotron Radiation Facility. All the XAFS spectra were analyzed by using the WinXAS version 3.1 program.[33] Then, the K-edge X-ray absorption near edge structure (XANES) spectra (from 25.497–25.597 keV) was selected for quantitative edge fitting analyses with the LSFitXAFS program.[34,35]

Osteogenic and Adipogenic Differentiation of Ag_2S QDs-Labeled hMSCs: Differentiation capacity of hMSCs with or without Ag_2S QDs-labeling was studied by adipogenic and osteogenic differentiation assays. For adipogenic differentiation, hMSCs were treated with adipogenic differentiation medium consisting of 1 μM dexamethasone (Sigma), 5 μg mL^{-1} insulin, 0.5 mM isobutyl-methylxanthine (IBMX) and 60 μM indometacin in the L-DMEM medium for up to 14 days. Cells were then fixed by 4% paraformaldehyde and stained with 0.36% Oil-Red O for 30 min. For osteogenic differentiation, hMSCs were treated with osteogenic supplements containing 100 nM dexamethasone, 0.05 mg mL^{-1} ascorbic acid, and 0.01 Mβ-glycerophosphate in the L-DMEM medium for up to 21 days. Osteogenic cells were determined by alizarin red staining. Both adipogenic and osteogenic cells were imaged by Nikon Ti-E microscopy.

In Vivo Detection Sensitivity of Ag_2S QDs-Labeled hMSCs: Ag_2S QDs-labeled hMSCs (10^5, 2×10^4, 10^4, and 10^3 cells) in 20 μL PBS were subcutaneously injected into the back of athymic nude mice. The NIR-II PL images of the mice were collected at day 0, 3, 8, 15, 20 and 30 days after injection. All the images were collected using a home-built NIR in vivo imaging system equipped with an InGaAs/SWIR camera (Photonic Science, UK), an 880 nm long-pass filter and an 1100 nm long-pass filter (Daheng Optics and Fine Mechanics Co., Ltd, China).[36] An 808 nm diode laser (Starway Laser Inc., China) was used as the excitation source. The laser power density was 123.8 mW cm^{-2} (beam size 106 cm^2) during imaging with an exposure time of 100 ms. The calibrated NIR fluorescent intensity of Ag_2S QDs-labeled hMSCs at different cell number were analyzed by imageJ2x software.

In Vivo Tracking of Ag_2S QDs-Labeled hMSCs in Mice with Acute Liver Failure: Female athymic nude mice (6 weeks old) were purchased from Suzhou Belda Bio-Pharmaceutical Corporation. Animal studies were performed under the guidelines approved by Soochow University Laboratory Animal Center. Mice with acute liver failure were prepared by an intraperitoneal injection of 0.1% CCl_4 (diluted in olive oil) at a dose of 10 μL g^{-1}. After 4 h, 1.5×10^6 Ag_2S QDs-labeled hMSCs suspended in 250 μL of PBS containing 5 U mL^{-1} heparin were intravenously injected via the tail vein into the acute liver failure mice. Meanwhile, healthy mice intravenously injected with 1.5×10^6 Ag_2S QDs-labeled hMSCs were prepared as the control group. For in vivo imaging studies, both the acute liver failure mice and healthy mice were monitored at multiple time points (20 min, 2 h, 6 h, 24 h, 7 days, and 14 days) using the NIR in vivo imaging system. All the images were collected with an exposure time of 100 ms.

Supporting Information

Supporting Information is available from the Wiley Online Library or from the author.

Acknowledgements

The authors thank the funding by Chinese Academy of Sciences "Bairen Ji Hua" program and "Strategic Priority Research Program" (XDA01030200), Ministry of Science and Technology of China (2011CB965004), National Natural Science Foundation of China (21073225), Natural Science Foundation of Jiangsu Province (BK2012007), and CAS/SAFEA International Partnership Program for Creative Research Teams.

Received: September 22, 2013
Revised: October 31, 2013
Published online: December 20, 2013

[1] B. Parekkadan, J. M. Milwid, *Annu. Rev. Biomed. Eng.* **2010**, *12*, 87.
[2] K. M. Dupont, K. Sharma, H. Y. Stevens, J. D. Boerckel, A. J. Garcia, R. E. Guldberg, *Proc. Natl. Acad. Sci. U. S. A.* **2010**, *107*, 3305.
[3] H. Yukawa, H. Noguchi, K. Oishi, S. Takagi, M. Hamaguchi, N. Hamajima, S. Hayashi, *Cell Transplant.* **2009**, *18*, 611.
[4] A. Banas, T. Teratani, Y. Yamamoto, M. Tokuhara, F. Takeshita, M. Osaki, M. Kawamata, T. Kato, H. Okochi, T. Ochiya, *Stem Cells* **2008**, *26*, 2705.
[5] L. C. Amado, A. P. Saliaris, K. H. Schuleri, M. St John, J. S. Xie, S. Cattaneo, D. J. Durand, T. Fitton, J. Q. Kuang, G. Stewart, S. Lehrke, W. W. Baumgartner, B. J. Martin, A. W. Heldman, J. M. Hare, *Proc. Natl. Acad. Sci. U. S. A.* **2005**, *102*, 11474.
[6] C. Villa, S. Erratico, P. Razini, A. Farini, M. Meregalli, M. Belicchi, Y. Torrente, *Tissue Eng. Part B: Rev.* **2011**, *17*, 1.
[7] H. Wang, F. Cao, A. De, Y. Cao, C. Contag, S. S. Gambhir, J. C. Wu, X. Y. Chen, *Stem Cells* **2009**, *27*, 1548.
[8] S. Kidd, E. Spaeth, J. L. Dembinski, M. Dietrich, K. Watson, A. Klopp, V. L. Battula, M. Weil, M. Andreeff, F. C. Marini, *Stem Cells* **2009**, *27*, 2614.
[9] Z. J. Li, Y. Suzuki, M. Huang, F. Cao, X. Y. Xie, A. J. Connolly, P. C. Yang, J. C. Wu, *Stem Cells* **2008**, *26*, 864-873.
[10] A. B. Rosen, D. J. Kelly, A. J. T. Schuldt, J. Lu, I. A. Potapova, S. V. Doronin, K. J. Robichaud, R. B. Robinson, M. R. Rosen, P. R. Brink, G. R. Gaudette, I. S. Cohen, *Stem Cells* **2007**, *25*, 2128.
[11] H. Yukawa, M. Watanabe, N. Kaji, Y. Okamoto, M. Tokeshi, Y. Miyamoto, H. Noguchi, Y. Baba, S. Hayashi, *Biomaterials* **2012**, *33*, 2177.
[12] C. Liang, C. Wang, Z. Liu, *Part. Part. Syst. Charact.* **2013**, DOI: 10.1002/ppsc. 201300199.
[13] L. Cheng, C. Wang, X. X. Ma, Q. L. Wang, Y. Cheng, H. Wang, Y. G. Li, Z. Liu, *Adv. Funct. Mater.* **2013**, *23*, 272.
[14] C. Wang, L. Cheng, H. Xu, Z. Liu, *Biomaterials* **2012**, *33*, 4872.
[15] P. Yi, G. Chen, H. Zhang, F. Tian, B. Tan, J. Dai, Q. Wang, Z. Deng, *Biomaterials* **2013**, *34*, 3010.
[16] C. Wang, X. X. Ma, S. Q. Ye, L. Cheng, K. Yang, L. Guo, C. H. Li, Y. G. Li, Z. Liu, *Adv. Funct. Mater.* **2012**, *22*, 2363.
[17] S. Magnitsky, D. J. Watson, R. M. Walton, S. Pickup, J. W. Bulte, J. H. Wolfe, H. Poptani, *Neuroimage* **2005**, *26*, 744.
[18] B. B. Chin, Y. Nakamoto, J. W. M. Bulte, M. F. Pittenger, R. Wahl, D. L. Kraitchman, *Nucl. Med. Commun.* **2003**, *24*, 1149.
[19] A. M. Smith, M. C. Mancini, S. Nie, *Nat. Nanotechnol.* **2009**, *4*, 710.
[20] K. Welsher, S. P. Sherlock, H. J. Dai, *Proc. Natl. Acad. Sci. U. S. A.* **2011**, *108*, 8943.
[21] G. S. Hong, J. C. Lee, J. T. Robinson, U. Raaz, L. M. Xie, N. F. Huang, J. P. Cooke, H. J. Dai, *Nat. Med.* **2012**, *18*, 1841.
[22] G. Hong, J. T. Robinson, Y. Zhang, S. Diao, A. L. Antaris, Q. Wang, H. Dai, *Angew. Chem. Int. Ed.* **2012**, *51*, 9818.
[23] Y. Du, B. Xu, T. Fu, M. Cai, F. Li, Y. Zhang, Q. Wang, *J. Am. Chem. Soc.* **2010**, *132*, 1470.

[24] Y. Zhang, G. S. Hong, Y. J. Zhang, G. C. Chen, F. Li, H. J. Dai, Q. B. Wang, *ACS Nano* **2012**, *6*, 3695.
[25] Y. Zhang, G. Hong, W. He, K. Zhou, K. Yang, F. Li, G. Chen, Z. Liu, H. Dai, Q. Wang, *Biomaterials* **2013**, *34*, 3639.
[26] A. M. Derfus, W. C. W. Chan, S. N. Bhatia, *Nano Lett.* **2004**, *4*, 11.
[27] Y. Qu, W. Li, Y. Zhou, X. Liu, L. Zhang, L. Wang, Y. F. Li, A. Iida, Z. Tang, Y. Zhao, Z. Chai, C. Chen, *Nano Lett.* **2011**, *11*, 3174.
[28] N. Chen, Y. He, Y. Su, X. Li, Q. Huang, H. Wang, X. Zhang, R. Tai, C. Fan, *Biomaterials* **2012**, *33*, 1238.
[29] H. Chibli, L. Carlini, S. Park, N. M. Dimitrijevic, J. L. Nadeau, *Nanoscale* **2011**, *3*, 2552.
[30] H. Yukawa, Y. Kagami, M. Watanabe, K. Oishi, Y. Miyamoto, Y. Okamoto, M. Tokeshi, N. Kaji, H. Noguchi, K. Ono, M. Sawada, Y. Baba, N. Hamajima, S. Hayashi, *Biomaterials* **2010**, *31*, 4094.
[31] Y. F. Wang, G. Y. Liu, L. D. Sun, J. W. Xiao, J. C. Zhou, C. H. Yan, *ACS Nano* **2013**, *7*, 7200.
[32] Y. Lei, H. Tang, L. Yao, R. Yu, M. Feng, B. Zou, *Bioconjug. Chem.* **2008**, *19*, 421.
[33] T. Ressler, *J. Synchrotron Radiat.* **1998**, *5*, 118.
[34] D. Paktunc, *J. Synchrotron Radiat.* **2004**, *11*, 295.
[35] G. C. Chen, X. C. Chen, Y. Q. Yang, A. G. Hay, X. H. Yu, Y. X. Chen, *Appl. Environ. Microb.* **2011**, *77*, 4719.
[36] C. Li, Y. Zhang, M. Wang, Y. Zhang, G. Chen, L. Li, D. Wu, Q. Wang, *Biomaterials* **2014**, *35*, 393.